# East West University

Spring -2017

Thesis Report

## "Design and Simulation of CdS/CIGS p-i-n high efficiency solar cell"

**Submitted by**

Dipta Halder
ID: 2013-1-55-027

SK Asifuddin
ID: 2013-1-55-011

Tasnim Esha

ID:2013-1-55-003

**Thesis Supervisor**
M. Mofazzal Hossain,Ph.D.
ProfessorDepartment of Electronics and Communications Engineering

# Declaration

We hereby declare that we have completed project on the topic entitled "Design and Simulation of CdS-CIGS p-i-n Solar Cell using TCO, Intrinsic and BSF Layers" as well as prepared as research report to the department of Electronics and Communications Engineering, East West University in partial fulfillment of the requirement for the degree of B.Sc. in Electronics and Telecommunications Engineering, under the course "Research/Internship (ETE 498)".

We further assert that this report in question is based on our original exertion having never been produced fully and/or partially anywhere for any requirement.

……………………..
Dipta Halder
ID: 2013-1-55-027

…………………….
SK Asifuddin
ID: 2013-1-55-011

&

……………………..
Tasnim Esha
ID: 2013-1-55-003

# Acceptance

This research report presented to the Department of Electronics and Communications Engineering, East West University is submitted in partial fulfillment of the requirement for the degree of B. Sc. In Electronics and Telecommunications Engineering, under complete supervision of the undersigned.

………………………………

M. Mofazzal Hossain,Ph.D.
Professor,
Department of Electronics and Communications Engineering

# Acknowledgement

First and foremost with all our heartiest devotion we are grateful to almighty Allah for blessing us with such opportunity of learning and ability to successfully complete the task.

A special thanks with honor to our supervisor M. Mofazzal Hossain who was kind enough to allocate his valuable time to provide us with his humble guidance, motivating thought and encouragement.

…………………………..
Dipta Halder
ID: 2013-1-55-027

………………………….
SK Asifuddin
ID: 2013-1-55-011

&

…………………………..
Tasnim Esha
ID: 2013-1-55-003

# Abstract

A high efficiency CdS/CIGS solar cell is designed using an intrinsic layer and a highly doped CdS as a back surface field (BSF) layer. With the combination of TCO layer (ZnO), CdS window layer, CIGS BSF layer, the higher conversion efficiency is achieved which is about 29.216% in simulation. After introducing intrinsic layer efficiency increased by great extent. In addition to this, with the increase of thickness of intrinsic layer efficiency also increased. At AM 1.5 solar radiations, the proposed cell structure had a $V_{oc}$ of 0.696 V, a $J_{sc}$ of 59.975 mAcm$^{-2}$, a maximum power is 34.945 mW/cm$^2$ and a fill factor of 84%, corresponding to an overall efficiency of 29.216%

# Index


| Contents | Page No |
|---|---|

# Chapter 1

## Introduction

### 1.1 Solar Energy

Solar energy is defined as energy obtained from the sun's radiation. It derived from the sun in the form of solar radiation. The two main forms of solar energy include active solar energy and passive solar energy. Active solar energy involves equipment or an action to convert solar energy into a usefulform. One example of active solar energy is the use of solar cells to convert energy from the sun into electrical energy that can be used in the home. Passive solar energy does not require anyspecific action or equipment. An example of passive solar energy is strategically placing windows in a home to allow sunlight to enter and provide heat. [1]

Solar energy can be harnessed using a range of technologiessuch as solar photovoltaic, solar heaters and solar thermalelectricity. It is considered an environmentally friendly source of energy because it comes directly from the sun; it does not involve the burning of fossil fuels. The primary limitation ofsolar energy is that it is not always available, and methods of storage and stop-gap are required for when it is cloudy ordaining outside. [2]Solar energy is a type of radiant energy, so named for the vibration particles 'radiating' from the sun. Solar energy is also called solar radiation for this reason. Solar energy also does other kinds of work indirectly. Plants use the sun's energy through the process of photosynthesis to grow and more indirectly. The sun is such an important part of life on Earth that it's not surprising that so many end-of-the world science fiction movies related with the sun not doing its job properly. Solar energy is important to support life on earth, it helps to grow our food, light our days, influence weather patterns, provide heat and can be used to generate solar electricity man-made devices such as solar panels or solar cells in order to provide a source of clean and low cost renewable energy. Solar energy technologies are becoming more advanced. Photons contained in this solar radiation makes the generation of electricity from the sun rays. Solar energy is also responsible for wind energy, as

wind patterns are very much influenced by the sun. Also, the sun is responsible for heating the ground beneath our feet to a significant degree to support the use of geothermal, ground source heat pumps.

## 1.2 Potential and Importance of Solar Energy

Solar energy is a major renewable energy source with the potential to meet many of the challenges facing the world.

Solar energy is a potential solution to the environmental problems being caused by fossil fuels. When fossil fuels are burned to generate electricity, they release harmful greenhouse gases into the atmosphere. The vast majority of scientists believe that continuing to depend on fossil fuels is going to cause serious environmental problems in the future. Another important use for solar energy is in satellites. Many satellites are engineered with photovoltaic panels, which capture sunlight and convert it into electricity that is used to power the satellite. Solar power is also useful in areas where standard electricity is not available. For example, research facilities in Antarctica depend on sustainable energy sources, such as the sun and wind turbines, to generate power. Emergency phone systems in remote places often use solar power as a dependable power source. Solar energy can also be used to power devices that run at night. For example, some streetlights are able to charge energy from the sun during the day, then run throughout the night. [3]

Some few importance of solar cell are:

1. Importance to Environmental Protection
2. Solar is clean and safe.
3. Prevents destruction of habitats.
4. Combat climate change.
5. Social and economic benefits.
6. Small and decentralized electricity source.
7. Cheap and reliable energy source.

**Fig 1.1: solar cell**

## 1.3 Generation of solar Energy

Solar energy is the most powerful of all renewable energy resources. The Earth's reserves of fossil fuels, such as petroleum and coal, may eventually be depleted. Moreover, burning these fossil fuels creates carbon dioxide emissions, which are suspected contributor to climate change. In contrast, as long as the sun exists, we can harness its energy here on Earth. Every second, the sun sends about 42 trillion kilocalories of energy to the Earth. If we could convert 100% of this solar energy into electricity, we could create one year's worth of power for the entire planet in a single hour. A solar power plant usually has a system of mirrors to concentrate the sunlight on to an absorber, the absorbed energy then being used to power a heat engine which in turn drives a rotary generator. In large scale systems, the heat engine is usually a turbine which is driven by steam or other vaporous working fluid. The thermal energy comes from the suns radiation and not from the air. As we know the temperature of air will usually be much lower than the temperature of the working fluid.

## 1.3.1 PV Solar cell:

PV cells are made from layers of semi-conducting material, usually silicon. When light shines on the cell it creates an electric field across the layers. The stronger the sunshine, the more electricity is produced. Groups of cells are mounted together in panels or modules that can either be mounted on your roof or on the ground.

The power of a PV cell is measured in kilowatts peak (kWp). That's the rate at which it generates energy at peak performance in full direct sunlight during the summer. PV cells come in a

varietyof shapes and sizes. Most PV systems are made up of panels that fit on top of an existing roof, but you can also fit solar tiles.

## 1.3.2 Thermal solar cell:

Solar water heating (known as solar thermal) systems capture the free heat from the sun and use it to heat up water for use in the home. It's a simple process:

- Panels on your roof absorb heat from the sun – they are known as the collector

- The water in the panels heats up

- This hot water is pumped through a coil in your cylinder

- Which transfers the heat to the water in the cylinder

## 1.4 Advantages of Solar Energy:

### 1.4.1 Renewable energy

One-time cost of acquiring a photovoltaic system and have it installed are relatively high.

The energy can be used both to generate electricity and heat in the house. Renewable energy is recovered from the sun, the wind and waves - which in this case is the sun. Solar cells harness the energy from the sun and transform this into usable electricity.

### 1.4.2 Infinite Energy

When you have the opportunity to extract energy from the sun's rays, this is a source of energy that will never be exhausted, therefore there will always be a source for electricity production..

### 1.4.3 Maintenance

Very little maintenance are needed to running a solar cell.

### 1.4.4 Pollution free

Solar cell causes zero pollution. Solar cell is clean and renewable energy source.

## 1.5 Disadvantage of Solar energy

### 1.5.1 High investment

### 1.5.2 Interior needs

Not all households that can satisfy their requirements and get the optimum out of their solar cells yet. Solar cells are very sensitive in terms of their location, which means that if there is shade on your lot, it is difficult to exploit solar installation optimally.

### 1.5.3Current conversion

A practical problem linked with the use of solar cell panels is regarding the storage of electricity general by them. The electricity generated by the solar cell panel is stored during the day with the help of storage batteries which give us only direct current. But to operate our devices we need alternating current. Therefore we need to convert DC to AC before using any appliance and thus it increases the cost of such solar panels as the sources of electricity.6 Types of Solar Cells There are three types of solar cells:

1. Water based PV cell

    a. Monocrystalline

    b. Polycrystalline

2. Thin film

    a. CdTe

    b. CIGS

3. Emerging PV cell
    a. QD solar cell
    b. Dye-senselized

**1.6 Types of solar cells**


**1. 6.1.a Monocrystalline**:

Monosilicon has higher efficiency and thus higher cost. Commercial monosilicon efficiency approximates 22% as produced by US and Japanese solar manufacturers. Crystalline silicon devices have theoretical limiting efficiency of 29% and can achieve an energy payback period of 1-2 years. Most of the low end manufacturers are producing polysilicon PV cells with efficiency of 7-8%. Monocrystalline panels are generally constructed from high-quality silicon, giving them the highest performance rates in the industry, usually up to 21%. By comparison, monocrystalline panels outperform thin film by four to one. They also make wise use of space, so they offer a high power yield per square foot. Some disadvantage of monocrystalline are they are high-quality, these panels are also costly. Circuit break down is common when the panel is obstructed or shaded. The manufacturing process produces significant waste. The panels perform best in warm weather, with performance decreasing as temperatures increase.

**1.6.1. b Polycrystalline:**

High temperature ratings are slightly lower than those for monocrystalline panels; however, the difference is minor, making these types of panels a good option for many homeowners. The manufacturing process produces little waste, and the technology allows for a cost-effective panel. Some disadvantage of polycrystalline are efficiency is lower, typically between 13% and 16%, which is not nearly as high as the ratings for monocrystalline panels.The panels require more space when installed to produce the same electrical output as a panel constructed from monocrystalline.


**1.6.2 Thin film:**

A thin-film solar cell is a second generation solar cell that is made by depositing one or more thin layers, or thin film (TF) of photovoltaic material on a substrate, such as glass, plastic or metal. These panels are lightweight, they are generally immune to problems from shading or obstructions and low-light conditions generally don't hinder their performance. These panels are easy to mass produce, so they are an affordable option.

Since the invention of the first modern silicon solar cell in 1954, incremental improvements have resulted in modules capable of converting 12 to 18% of solar radiation into electricity.

Cells made from these materials tend to be less efficient than bulk silicon, but are less expensive to produce. Their quantum efficiency is also lower due to reduced number of collected charge carriers per incident photon.

The performance and potential of thin-film materials are high, reaching cell efficiencies of 12–20%; prototype module efficiencies of 7–13%; and production modules in the range of 9%. The thin film cell prototype with the best efficiency yields 20.4% (First Solar), comparable to the best conventional solar cell prototype efficiency of 25.6% from Panasonic.

### 1.6.2.a CdTe Technology

The most common CdTe solar cells consist of a simple p-n heterojunction structure containing a p-doped CdTe layer matched with an n-doped cadmium sulfide (CdS) layer, which acts as a window layer. This structure is similar to the heterojunction in CIGS cells. As with most thin-film solar technologies, carrier collection is accomplished by drift, or field-assisted collection.

Typical CdTe thin-film deposition techniques include: close-spaced sublimation, vapor-transport deposition, and physical-vapor deposition, sputter deposition, electrodeposition, and metal-organic chemical-vapor deposition, spray deposition, and screen-print deposition.CdTe solar cells are completed by adding a high-quality transparent conductive oxide (TCO)—usually fluorine-doped tin oxide ($SnO_2$:F)—and a back electrical contact—typically a metal or carbon paste with copper (Cu). One disadvantage to using Cu in the back contact is the gradual diffusion of Cu atoms into the CdTe and CdS layers, which creates defects and promotes Cu accumulation at the CdTe/CdS junction.

Overall CdTe solar cell performance was significantly improved after the discovery of a cadmium chloride ($CdCl_2$) vapor treatment. This annealing process is accomplished in the presence of oxygen at temperatures near 390°C after the CdTe layer is grown on the CdS layer and prior to the back-contact deposition. The $CdCl_2$ treatment has positive effects on the CdTe solar cell, such as growth of larger CdTe grains and the passivation of defects.

7

**1.6.2.b CIGS technology**

Several prominent manufacturers couldn't stand the pressure caused by advances in conventional c-Si technology of recent years. The company Solyndra ceased all business activity and filed for Chapter 11 bankruptcy in 2011, and Nanosolar, also a CIGS manufacturer, closed its doors in 2013. Although both companies produced CIGS solar cells, it has been pointed out, that the failure was not due to the technology but rather because of the companies themselves, using a flawed architecture, such as, for example, Solyndra's cylindrical substrates. In 2014, Korean LG Electronics terminated research on CIGS restructuring its solar business, and Samsung SDI decided to cease CIGS-production, while Chinese PV manufacturer Hanergy is expected to ramp up production capacity of their 15.5% efficient, 650 mm×1650 mm CIGS-modules. One of the largest producers of CIGS photovoltaics is the Japanese company Solar Frontier with a manufacturing capacity in the gigawatt-scale.

The benefits of CIGS solar cells include:

- **High absorption**: This direct-band gap material can absorb a significant portion of the solar spectrum, enabling it to achieve the highest efficiency of any thin-film technology.
- **Tandem design**: A tunable band gap allows the possibility of tandem CIGS devices.
- **Protective buffer layer**: The grain boundaries form an inherent buffer layer, preventing surface recombination and allowing for films with grain sizes of less than 1 micrometer to be used in device fabrication.

**1.6.3 Emerging PV cell**

The definition of third generation technology, however, is less clear, with the moniker "third generation" usually reserved for so-called emerging technologies. This group is sometimes described as including any technology capable of overcoming the Shockley–Queisser limit of power conversion efficiency (33.7 percent) for a single junction device. Most technologists would also include broad classes of other conversion devices including non-semiconductors such as polymer and dye-sensitized cells, tandem cells built from stacks of conventional materials (such as amorphous silicon or gallium arsenide), and nanotechnology. For an introduction to the various types of photovoltaic materials and cells, see the previous TechZone article *"Solar Cell and Photovoltaic Primer."*

### 1.6.3.a QD solar cell

Quantum dots have offered an attractive option for photovoltaics. Multijunction solar cells made from colloidal quantum dots (CQD) have been able to achieve around 7-percent conversion efficiency in the lab. While figures like this may not seem too impressive when compared to silicon solar cells, their promised theoretical conversion efficiency limit is an eye-popping 45 percent. This is possible because when a single photon is absorbed by a quantum dot, it produces more than one bound electron-hole pair, or exciton, thereby doubling normal conversion efficiency numbers seen in single-junction silicon cells.

Now researchers at the Massachusetts Institute of Technology (MIT) have raised. Furthermore, says the MIT team, it can be produced using an inexpensive production method that promises to keep manufacturing costs down.[4]

### 1.6.3.b Dye-senselized

Dye solar cells (DSCs) which are discussed in this application note are thin film cells. They are also called dye sensitized solar cells (DSSC) or Grätzel cells named after the Swiss chemist Michael Grätzel who was greatly involved in the development of new cell types. Manufacturing of DSCs is simple, mostly low cost, and incorporate environmentally friendly materials. They have a good efficiency (about 10-14 %) even under low flux of sunlight. However, a major drawback is the temperature sensitivity of the liquid electrolyte. Hence a lot of research is going on to improve the electrolyte's performance and cell stability.
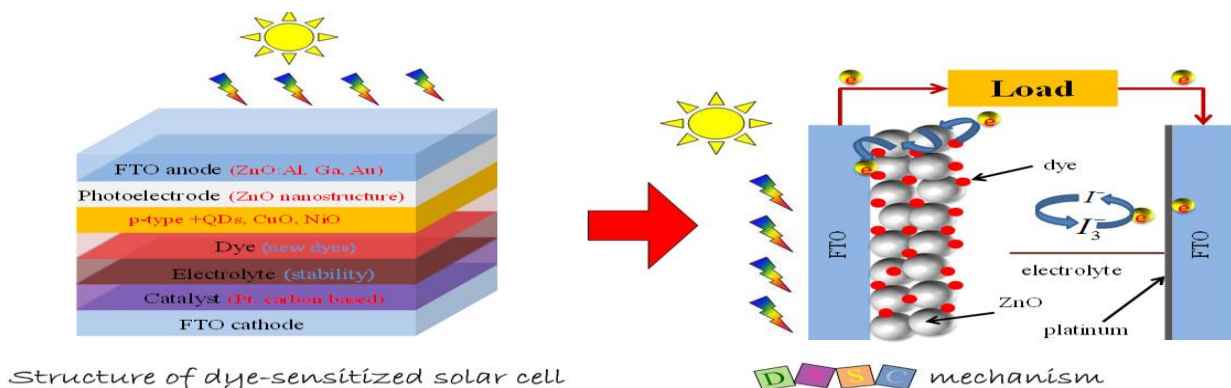


Fig 1.2: Structure of dye-sensitized solar cell

## 1.7 Thesis Layout

In summary, the purpose of this research is

1. To design a highly efficient five-layered CIGS solar cell

2. To optimize the layer thickness and doping density of BSF layer

3. To optimize the layer thickness of TCO layer

4. To optimize the layer thickness of intrinsic layer

5. To simulate the whole design using SILVACO software

Reference:

1. www.reference.com/science/definition-solar-energy-bd63bb5a85cb22a1#
2. www.reference.com/science/solar-energy-e50b3783dfde1d72#
3. www.reference.com/science/solar-energy-important-323345a2f5340b84?qo=contentSimilarQuestions#
4. spectrum.ieee.org/nanoclast/green-tech/solar/quantum-dot-solar-cells-break-conversion-efficiency-record

# Chapter 2

# Methodology

In this work we designed a thin film solar cell including intrinsic layer. The structure of the cell is designed and simulated by the general-purpose ATLAS device simulator by Silvaco Inc. Here, the electrical characteristics of a solar cell based on virtual fabrication of its physical structure, allowing for direct manipulation of materials, dimensions and doping. Through simulation we predicted the efficiency, open circuit voltage, current density and fill factor. The operation of the ATLAS software is described in detail and our model is applied to known single junction cell designs.

## 2.1 Models

**To simulate designed cell, following mathematical models are included.**

## 2.1.1 Concentration Dependent Mobility (CONMOB)

CONMOB specifies that a concentration dependent mobility model be used for silicon and gallium arsenide. This model is a doping versus mobility table valid for 300K only.

## 2.1.2 Shockley-Read-Hall (SRH) Recombination

The Shockley-Read-Hall recombination is modeled as follows:

$$R_{SRH} = \frac{pn - n_{ie}^2}{TAUPO\left[n + n_{ie}\exp\left(\frac{ETRAP}{kT_L}\right)\right] + TAUNO\left[p + n_{ie}\exp\left(\frac{-ETRAP}{kT_L}\right)\right]} \qquad \textbf{[2.1]}$$

Where,

ETRAP = The difference between the trap energy level and the intrinsic Fermi level

11

TAUN0 = The electron lifetimes

TAUP0 = The hole lifetimes.

This model is activated by using the SRH parameter of the MODELS statement. The electron and hole lifetime parameters, TAUN0 and TAUP0, are user-definable in the MATERIAL statement. The default values for carrier lifetimes are shown in Table 2.1. Materials other than silicon will have different defaults values.

**Table 2.1** Parameter

| Statement | Parameter | Default | Units |
|-----------|-----------|---------|-------|
| MATERIAL | ETRAP | 0 | eV |
| MATERIAL | TAUNO | $1 \times 10^{-7}$ | s |
| MATERIAL | TAUPO | $1 \times 10^{-7}$ | s |

The constant carrier lifetimes that are used in the SRH recombination model above can be made a function of impurity concentration using the following equation:

$$R_{SRH} = \frac{pn - n_{ie}^2}{\tau_p \left[ n + n_{ie} \exp\left(\frac{ETRAP}{kT_L}\right) \right] + \tau_n \left[ p + n_{ie} \exp\left(\frac{-ETRAP}{kT_L}\right) \right]}$$ **[2.2]**

Where,

$$\tau_n = \frac{TAUNO}{AN + BN\left(\frac{N_{total}}{NSRHN}\right) + CN\left(\frac{N_{total}}{NSRHN}\right)^{EN}}$$ [2.3]

$$\tau_p = \frac{TAUPO}{AP + BP\left(\frac{N_{total}}{NSRHN}\right) + CN\left(\frac{N_{total}}{NSRHN}\right)^{EP}}$$ [2.4]

Here,

$N$ = The local impurity concentration.

The TAUN0, TAUP0, NSRHN, and NSRHP parameters can be defined on the MATERIAL statement.

**Table 2.2** Material properties

| Statement | Parameter | Default | Units |
|-----------|-----------|---------|-------|
| MATERIAL | TAUNO | 1 | S |
| MATERIAL | NSRHN | $-1\times10^3$ | $cm^{-3}$ |
| MATERIAL | TAUPO | 1 | s |
| MATERIAL | NSRHP | $-1\times10^3$ | $cm^{-3}$ |
| MATERIAL | AN | 1 | |
| MATERIAL | AP | 1 | |
| MATERIAL | BN | 0 | |
| MATERIAL | EP | 0 | |

## 2.1.3 Fermi-Dirac (FERMI)

**Fermi-Dirac reduced carrier concentrations in heavily doped regions.** Electrons in thermal equilibrium at temperature $T_L$ with a semiconductor lattice obey Fermi-Dirac statistics. That is the probability $f(\varepsilon)$ that an available electron state with energy $\varepsilon$ is occupied by an electron is:

$$f(\varepsilon) = \frac{1}{1+\exp\left(\frac{\varepsilon-E_F}{kT_L}\right)} \qquad [\mathbf{2.5}]$$

Where,

$E_{F} =$ A spatially independent reference energy known as the Fermi level

$k =$ is Boltzmann's constant.

If $\varepsilon - E_F \gg kT_L$, then the above equation can be express as,

$$f(\varepsilon) = \exp\left(\frac{\varepsilon - E_F}{kT_L}\right)$$

[**2.6**]

## 2.1.4 Auger Recombination

Auger recombination occurs through a three particle transition whereby a mobile carrier is either captured or emitted. It is important at high current densities. The underlying physics for such processes is unclear and normally a more qualitative understanding is sufficient.

Auger Recombination is commonly modeled using the expression:

$R_{Auger} = AUGN (pn^2 - nn^2_{ie}) + AUGP (np^2 - pn^2_{ie})$            [**2.7**]

Where the model parameters AUGN and AUGP are user-definable in the MATERIAL statement.

**Table 2.3** Parameter for Equation [2.7]

| Statement | Parameter | Value | Units |
|-----------|-----------|-------|-------|
| MATERIAL | AUGN | 0 | $cm^6/s$ |
| MATERIAL | AUGP | 0 | $cm^6/s$ |

## 2.1.5 Bandgap Narrowing (BGN)

In the presence of heavy doping, greater than $10^{18} cm^{-3}$, experimental work has shown that the pn product in silicon becomes doping dependent. As the doping level increases, a decrease in the bandgap separation occurs, where the conduction band is lowered by approximately the same amount as the valence band is raised. In ATLAS this is simulated by a spatially varying intrinsic concentration $n_{ie}$ defined according to equation

$n^2_{ie} = n^2_i \exp\left(\frac{\Delta Eg}{kT}\right)$            [**2.8**]

Band gap narrowing effects in ATLAS are enabled by specifying the BGN parameter of the MODELS statement. These effects may be described by an analytic expression relating to the variation in bandgap, $\Delta Eg$, to the doping concentration, N. The expression used in ATLAS is from Slot boom and de Graaf:

14

$$\Delta Eg = BGN.E\left\{ ln\frac{N}{BGN.N} + \left[ \left( ln\frac{N}{BGN.N} \right)^2 + BGN.C \right]^{\frac{1}{2}} \right\}$$

**[2.9]**

We can specify the BGN.E, BGN.N, and BGN.C parameters in the MATERIAL statement. The default values from Slot boom and Klaassen are shown in Table 2.3.

**Table 2.3** Parameters for Bandgap Narrowing Model

| Statement | Parameter | Values | Unit |
|-----------|-----------|--------|------|
| MATERIAL | BGN.E | 0.009 | eV |
| MATERIAL | BGN.N | $1\times10^{17}$ | $cm^{-3}$ |
| MATERIAL | BGN.C | 0.5 | - |

## 2.1.6 Optical Generation/Radiative Recombination

OPTR selects the optical recombination model. When this parameter is specified, the COPT parameter of the MATERIAL statement should be specified. The next physical mechanisms we have to consider for generation/recombination are photon transition. There are two partial processes involved. For radiative recombination, an electron loses energy on the order of the band gap and moves from the conduction band to the valence band. For optical generation, an electron moves from the valence band to the conduction. In silicon, band to band generation/recombination is insignificant. This effect, however, is important for narrow gap semiconductors and semiconductors whose specific band structure allows direct transitions. By assuming a capture rate CcOPT and an emission rate CeOTP, the involved partial processes can be written as:

$$R_{np}^{OPT} = C_c^{OPT}{}_{np}$$

**[2.10]**

for recombination and

$$G_{np}^{OPT} = C_e^{OPT}$$

**[2.11]**

for generation

These rates must be equal in thermal equilibrium so that

$$C_{np}^{OPT} = C_c^{OPT} n_{ie}^2 \qquad\qquad \textbf{[2.12]}$$

The total band to band generation/recombination is the difference of the partial rates, which equates to

$$R_{np}^{OPT} = C_c^{OPT}(np - n_{ie}^2) \qquad\qquad \textbf{[2.13]}$$

In ATLAS, COPT is used express $C_c^{OPT}$ and can be defined away from default values on the materials statement or implemented using a C-Interpreter routine.

## 2.2 Simulating Photodetectors

### 2.2.1 Defining Optical Sources

We can define up to ten optical sources. Optical sources are described by using the BEAM statement. All BEAM statements must appear somewhere after the MESH, REGION, DOPING, and ELECTRODE statements and before any SOLVE statement. The parameters in the BEAM statement describe a single optical source.

The NUM parameter is used to uniquely identify one optical source. Values between 1 and 10 are valid for the NUM parameter. Optical sources are subsequently referred to by the value of their NUM parameter. The ANGLE parameter specifies the angle of the direction of propagation of the beam with respect to the device coordinate system. ANGLE=90 specifies vertical (normal) illumination from above.

The optical source can be either monochromatic or multispectral. For monochromatic sources, we can use the WAVELENGTH parameter to assign the optical wavelength. WAVELENGTH uses the unit microns to be more consistent with the rest of ATLAS. For multispectral sources, spectral intensity is described in an external ASCII file indicated by the POWER.FILE parameter. This is a text file that contains a list of pairs defining wavelength and spectral intensity. The first line of the file gives the integer number of wavelength-intensity pairs in the file. An example of such a file is shown below.

```
4
0.4 0.5
0.5 1.0
0.6 1.2
```

16

0.7 1.1

This example specifies that there are four samples and that at a wavelength of 0.4 μm, the intensity is 0.5 Watts per square cm per μm of wavelength, and so on. With multispectral sources, specify a discretization of the interpolated information. Values must be specified for the WAVEL.START, WAVEL.END, and WAVEL.NUM parameters. These values specify the starting and ending wavelengths and the number of wavelengths to sample. LUMINOUS uses wavelengths at equal intervals over a specified range of wavelengths. LUMINOUS performs an independent ray trace at each of the sample wavelengths. For example:

WAVEL.START=0.4 WAVEL.END=0.6 WAVEL.NUM=2

Causes ray traces at wavelengths of 0.45 and 0.55. LUMINOUS obtains the intensity associated with each sample by integrating the values of the spectral intensity file using a piece wise linear approximation. Each integral is performed over the range between successive midpoints. In the preceding example, the integration for the sample at 0.45 would be performed over the range of 0.4 to 0.5.

For a multispectral source, the generation rate is given by:

$$G = \eta_0 \int_{WAVEL.START}^{WAVEL.END} \frac{P(\lambda)L\lambda}{hc} \, \alpha e^{-\alpha Y} d\lambda \qquad \textbf{[2.14]}$$

Where,

$\eta_0$ = The internal quantum efficiency.

$P(\lambda)$ = The power spectral density of the source.

L = A factor representing the cumulative loss due to reflections, transmissions, and absorption over the ray path.

$\lambda$ = The wavelength.

h = Planck's constant.

c = The speed of light.

$\alpha$ = The absorption coefficient

y = The depth of the device, where x,y forms the two-dimensional mesh.

WAVEL.START= The starting of spectral limits specified on the BEAM statement

WAVEL.END = The ending of spectral limits specified on the BEAM statement.

The source photocurrent is given by:

$$I_S = q\frac{Bn}{hc} W \int_{WAVEL.START}^{WAVEL.END} P(\lambda)\lambda d\lambda \qquad\qquad \textbf{[2.15]}$$

Where,

P($\lambda$) = The power spectral density of the source.

The other parameters have the same definition as in Equation

The available photo current is given by:

$$I_A = q\frac{Bn}{hc} \sum_{i=1}^{Nr} Wr \int_0^{Xi} \int_{WAVEL.START}^{WAVEL.END} P(\lambda)\ \alpha_i e^{-\alpha_i y} P_i dy d\lambda \qquad\qquad \textbf{[2.16]}$$

where

P($\lambda$) = The power spectral density of the source.

The other parameters have the same definition as in Equation.

LUMINOUS allows you to choose the units of spectral intensity in an input spectrum file. By default, the units of spectral intensity in the POWER.FILE are W/cm$^2$. In this case, LUMINOUS carries out the integration. If the units of spectral intensity in the POWER.FILE are W/cm2, then you need to use the flag INTEGRATE on the BEAM statement. In this case, each value P($\lambda$) in the second column of the file is a total intensity for a corresponding spectral interval. Integrals over spectrum are reduced to summations of P($\lambda$) values. In both cases, LUMINOUS treats the subsequently specified value of B on the SOLVE statement as a unit less multiplier or scale factor for intensity.

One of the simpler tasks in characterizing a photo detector design is to measure DC detection efficiency. This will be done typically as a function of bias voltage, optical intensity, or wavelength. Each of these analyses can be performed using the SOLVE statement. The Bn

18

parameter can be used to set the optical intensity of the optical sources described in the previous section. The following example illustrates obtaining a solution with a specified optical intensity:

SOLVE B1=1.0

This specifies that a solution is to be obtained for an optical intensity in the beam numbered "1" of 1.0 Watt/cm$^2$. If this were the first SOLVE statement specified, the ray trace in LUMINOUS would be initiated. At the start of the solution, the optical intensities of each optical source with a positive intensity is printed. In addition, the available photocurrent and source photocurrent are printed.

The available photocurrent divided by the source photocurrent is a measure of the external quantum efficiency of the detector. The calculated terminal current can be divided by the source or available photocurrents are used to evaluate the internal quantum efficiency of the device. To obtain $V_{OC}$ and $I_{SC}$ for a solar cell, first define the illumination conditions. This should be done as discussed above in describing multi-spectral sources. The short circuit current is obtained by defining the contacts as voltage dependent contacts (default) and obtaining a solution with the device under zero bias with illumination. This can typically be done as a first step by the following input statement, for example:

SOLVE B1=1

In this statement, it's assumed the source, B1, has been already defined and the intensity is expected in the actual device. When you obtain a solution, the terminal currents represent the short circuit current. The open circuit voltage is obtained by defining one or more of the contacts as current controlled.

This is done using the CONTACT statement. For example:

CONTACT NAME=anode

The response of photo detectors to angle of incidence can be obtained in a manner analogous to the method used to obtain spectral response. In this case, the ANGLE parameter of the SOLVE statement specifies an angle added to the value of the BEAM parameter PHI (ANGLE). This allows collection of response versus angle.

The following examples statements demonstrate the syntax.

SOLVEB1=1 ANGLE=0

SOLVEB1=1 ANGLE=10

SOLVEB1=1 ANGLE=20

SOLVEB1=1 ANGLE=30

SOLVEB1=1 ANGLE=40

SOLVEB1=1 ANGLE=50

SOLVEB1=1 ANGLE=60

Equivalently, you may find it more convenient to specify an angle ramp. To specify a ramp of angle, you should assign the BEAM parameter to the beam index of the optical source to be ramped. Also, you should specify the initial angle with the ANGLE parameter, the final angle with the AFINAL parameter, and the angle step size with the ASTEP parameter as illustrated in the following.

SOLVE B1=1 BEAM=1 ANGLE=0.0 ASTEP=10.0 AFINAL=60.0

This is completely analogous to the seven statements described above.

Luminous 2D provides flexible means for defining multispectral sources. In addition, you can directly access built-in public domain solar spectra for am0 and am1.5 conditions by specifying AM0 or AM1.5 on the BEAM statement. These spectra consist of numerous samples.

The following is an example of how you might define the BEAM statement for analysis of am1.5 conditions with sub sampling.

BEAM NUM=1 AM1.5 WAVEL.START=0.3 WAVEL.END=1.0 WAVEL.NUM=50

Here, we are choosing to simulate am1.5 conditions sampled between 0.3 microns and 1.0 microns at 50 samples. We do not have to worry about sampling the many peaks and valleys in the solar spectrum as it is automatically integrated into each subsample. The sub sampling effectsonly the number of wavelengths for which the propagation model is calculated not the integrated intensity. Ray tracing is the principal propagation model for cases where we are not concerned about interference or diffraction effects in the bulk of the device. This is most useful for relatively thick bulk devices, such as crystalline silicon devices. It is useful for planar or textured devices. For textured devices, the texturing must be described explicitly in the device structure. The following gives an example of the specification of ray tracing for the optical propagation model for Luminous.

BEAM NUM=1 AM1.5 WAVEL.START=0.3 WAVEL.END=1.0 WAVEL.NUM=50

In this case, we will perform 50 ray traces. The omission of other model keywords, such as TR.MATRIX, FDTD, or BPM, signifies that ray tracing will be performed.

For Luminous, the algorithm automatically traces exactly the right number of rays to completely resolve all discontinuities at the surface and deep into the device. Here, we will describe how to extract the most common figures of merit for solar cells. These extraction methods are solution strategies placed in your input deck after defining the device structure, physical models, and the optical source as described in the previous section.

Typically, the first step in solar analysis is to illuminate the device. You can turn on the illumination by assigning the beam intensity on a SOLVE statement as follows:

SOLVE B1=1.0

Here, we assign a value of one "sun" to the intensity of the optical source indexed as number

"1" (B1).

As we had assigned AM1.5 on the BEAM statement, this corresponds to standard test conditions. In some cases, we may encounter convergence difficulties and may need to ramp the light intensity as shown in the following:

SOLVE B1=1.0

You may also choose to assign the beam intensity to a value greater than one to simulate solar concentrator effects. Since we have not yet assigned any bias voltages, the current in the run time output corresponds to the short circuit current (Isc).

## 2.2.2 Air Mass

Air mass is a measure of how much atmosphere the sun's rays have to pass through on their way to the surface of the earth. The Air Mass quantifies the reduction in the power of light as it passes through the atmosphere and is absorbed by air and dust. The Air Mass is defined as:

$$AM = \frac{1}{cos(q)} [2.17]$$

Where,
q= The angle from the vertical (zenith angle)

When the sun is directly overhead, the Air Mass is 1.
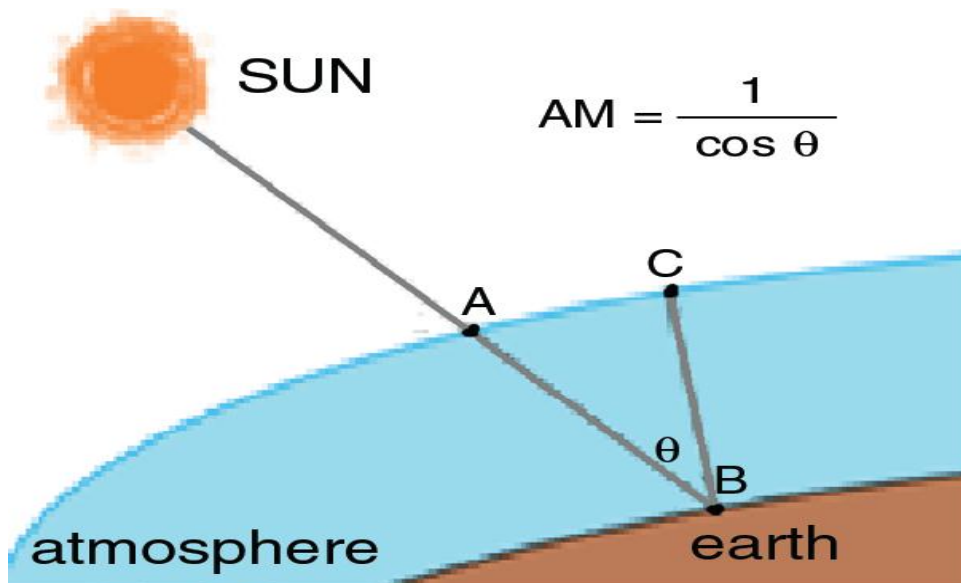


Air Mass is a measure of the amount of atmosphere the Sun's rays have to pass through. Air mass is abbreviated to AM where the following notation is used: AM1 is the amount of atmosphere the Sun's rays have to pass through when the Sun is directly overhead. This is the lowest possible AM value. In the example above where we had the Sun at 45° above the horizon, we write that we have AM1.41.As the Sun moves closer to the horizon, the amount of air mass that it's rays

22

have to pass through starts to rapidly increase. Here is a table of air mass for some values of solar zenith angle:

**Table2.4:** Different air mass ratio for different angle.

| SEA | Air Mass |
|-----|----------|
| 90° | AM1 |
| 60° | AM1.15 |
| 45° | AM1.41 |
| 30° | AM2 |
| 20° | AM2.92 |
| 15° | AM3.86 |

The "Standard" for testing. The air mass coefficient is defined in proportion to the cosine of the zenith angle (z): the angle between the beam from the Sun and the normal vector pointing directly up to the zenith of the sky (normal to the horizontal surface).

AM=1/cos(z) [simple, parallel plate]

One needs:

- The day number (N),
- The declination ($\delta$),
- The hour angle ($\omega$), and
- The local latitude ($\phi$) to calculate the zenith angle.
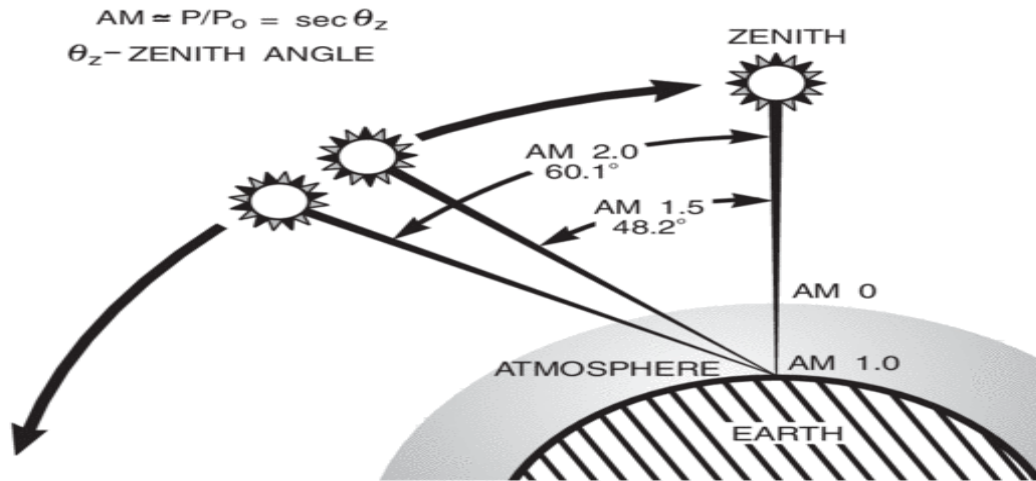


**Fig2.1:** Air Mass Ratio

An easy method to determine the air mass is from the shadow of a vertical pole. Let us assume that Object length is h, and shadow length is s. Air mass is the length of the hypotenuse divided by the object height h, and from Pythagoras's theorem we get:

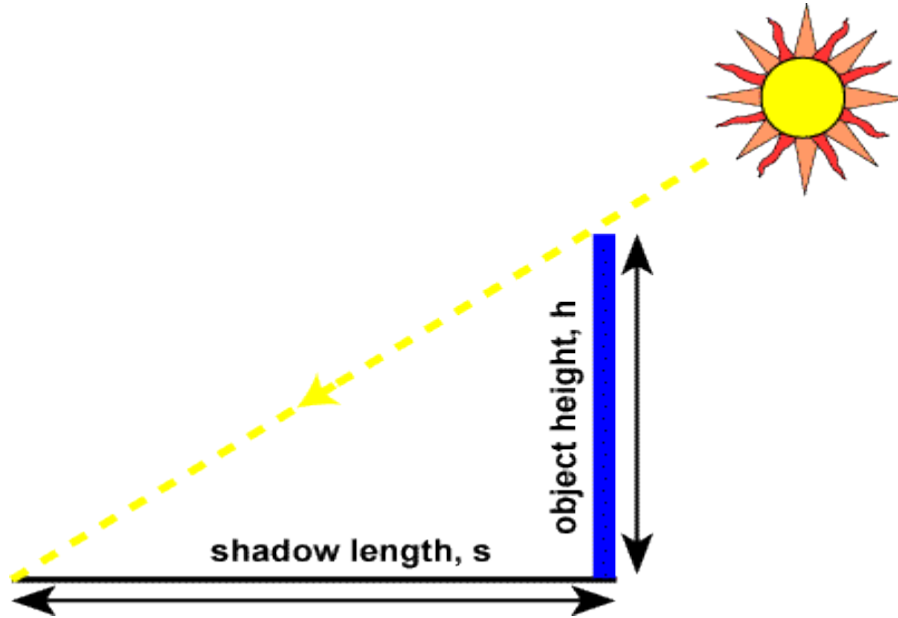$$AM= \sqrt{1 + (\tfrac{s}{h})^2} \qquad\qquad\qquad [2.18]$$



Figure 2.2: Air mass ratio using shadow length and object length

As the Sun get's closer to the horizon, the following equation can be used:

$$AM=\frac{1}{cosz + 0.50572(96.07995-z)^{-1.6364}} \qquad\qquad [2.19]$$

Where $z$ is (90 - solar zenith angle).
If the atmosphere is treated as a simple spherical shell, the above equation can be simplified to:

$$AM= \sqrt{(rcosz)^2 + 2r + 1} - rcosz \qquad\qquad [2.20]$$

Where again $z$ is (90 − solarzenith angle), and $r$ is the ratio the radius of the Earth (approx 6371km) to the depth of the atmosphere (9km since we can ignore the effect of the very thin atmosphere above that height without losing much accuracy). Therefore the value of $r$ is approximately 708.Using either of these equations, we see (approximately) that with an SEA of

10° we have AM5, at 5° we have AM10, at 2° we have AM20, and at 0° we have AM38. Therefore, when the Sun is say 2° above the horizon, the sunlight has to travel through 20 times more air mass than when the Sun is directly overhead.

The standard spectrum outside the Earth's atmosphere is called AM0, because at no stage does the light pass through the atmosphere. This spectrum is typically used to predict the expected performance of cells in space.

# Chapter 3

# Simulation Result & Discussion

## 3.1 Proposed Solar Cell

In a thin film solar cell there are several layers such as font and back contacts, transparent conductive oxide (TCO) layer, window layer (n-type), intrinsic layer, graded absorber layer (p-type) and back surface field (BSF) layer ($p^+$ type). In this solar cell we used Aluminium (Al) at the font contact, n-doped CdS at the window layer, CIGS at the both intrinsic and absorber layer as i-CIGS and p-CIGS and for the BSF layer we also used CIGS define as $p^+$-CIGS and molybdenum (Mo) at the back contact. The above describe cell is implemented in Silvaco software [9] and then simulated. The structure of the cell is shown in Fig.3.1.
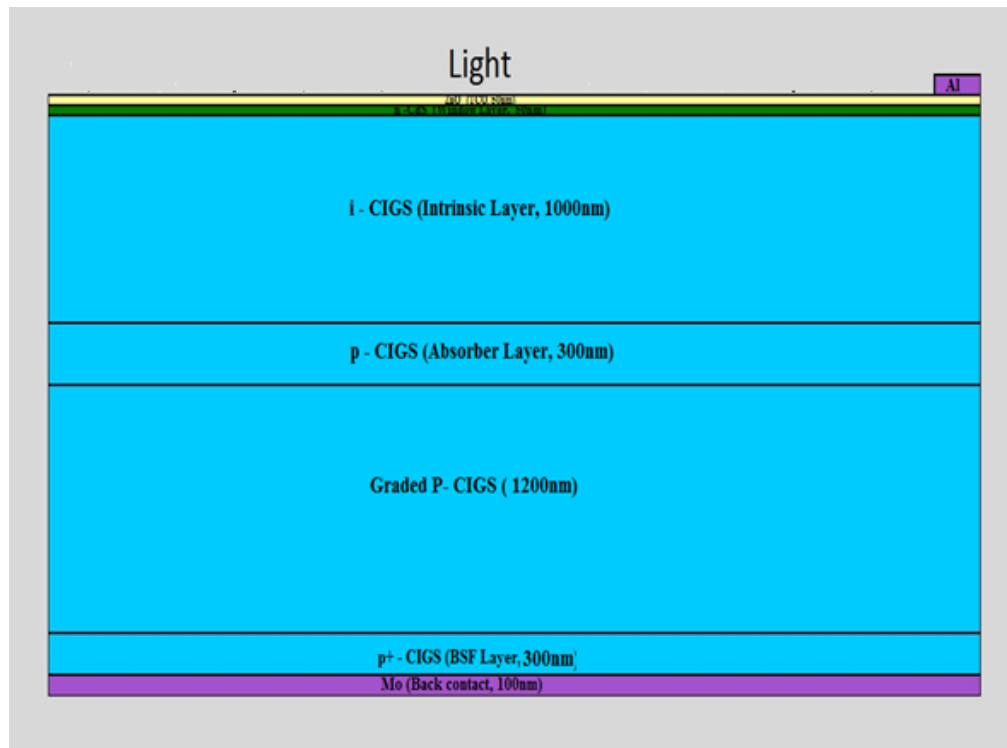


**Fig-3.1**: Proposed Solar Cell

## 3.2 Parameters of Different Layers

Parameters that are used in this project analysis for different layer and material are given as follow:

**Table-3.1**: TCO Layer Parameters

| No | Parameters | Value |
|----|------------|-------|
| 1 | Layer | TCO |
| 2 | Type | ZnO |
| 3 | Thickness (nm) | 50 |
| 4 | Eg(eV) | 3.37 |
| 5 | EPS | 8.49 |
| 6 | Nc (per cc) | $2.2 \times 10^{18}$ |
| 7 | Nv (per cc) | $1.8 \times 10^{19}$ |
| 8 | ni (per cc) | $3.11 \times 10^{-10}$ |

**Table-3.2**: Intrinsic Layer Parameters

| No | Parameters | Value |
|----|------------|-------|
| 1 | Layer | Intrinsic |
| 2 | Type | CIGS |
| 3 | Thickness (nm) | 100 |
| 4 | Eg(eV) | 1.07 |
| 5 | EPS | 13.6 |
| 6 | Nc (per cc) | $2.2 \times 10^{18}$ |
| 7 | Nv (per cc) | $1.8 \times 10^{19}$ |
| 8 | ni (per cc) | $6.57 \times 10^{9}$ |

**Table-3.3**: n Layer Parameters

| No | Parameters | Value |
|---|---|---|
| 1 | Layer | n-type |
| 2 | Type | CdS |
| 3 | Thickness (nm) | 50 |
| 4 | Eg(eV) | 2.48 |
| 5 | EPS | 10 |
| 6 | Nc (per cc) | $2.41 \times 10^{18}$ |
| 7 | Nv (per cc) | $2.57 \times 10^{19}$ |
| 8 | ni (per cc) | 0.0116 |

**Table-3.4**: P Layer Parameters

| No | Parameters | Value |
|---|---|---|
| 1 | Layer | p-type |
| 2 | Type | CIGS |
| 3 | Thickness (nm) | 300 |
| 4 | Eg(eV) | 1.07 |
| 5 | EPS | 13.6 |
| 6 | Nc (per cc) | $2.2 \times 10^{18}$ |
| 7 | Nv (per cc) | $1.8 \times 10^{19}$ |
| 8 | ni (per cc) | $6.57 \times 10^{9}$ |

## 3.3 TCO Layer

Transparent conductive oxides (TCO) are doped metal oxides used in optoelectronic devices such as flat panel displays and photovoltaic. A TCO is used as a front contact in order to create the heterojunction with the absorber and to gain as much photocurrent as possible from the solar panel with increasing the energy gap of the window layer. This layer should allow the largest possible percentage of photons to reach the absorber layer and is required for good conductivity

28

and high transmittance in visible light. Conductivity depends on the concentration and mobility of charge carriers, and its increase is usually achieved after mixing with elements such as Al. However, increasing the concentration of impurities using alloys leads to the reduction of the permeability of films at long wavelengths. Therefore, an increase in the mobility of carriers should be performed primarily by improvement of the film's crystalline. However, ZnO is considered the most competitive in cost and properties. Typically, these applications use electrode materials that have greater than 80% transmittance of incident light as well as electrical conductivities higher than 103 S/cm for efficient carrier transport. In general, TCOs for use as thin-film electrodes in solar cells should have a minimum carrier concentration on the order of $10^{20}$ cm$^{-3}$ for low resistivity and a band gap greater than 3.2 eV to avoid absorption of light over most of the solar spectra. Mobility in these films is typically limited by ionized impurity scattering due to the large amount of ionized donors in the order of 40 cm$^2$/(V·s) for the best performing TCOs

A good TCO has a large enough band gap to allow a majority of photons to reach the absorber layer. It is also critical that the TCO has a low resistivity to reduce recombination losses. This material boasts a low resistivity of ~$10^{-4}$Ω·cm and a transmittance of greater than 80%. In common CIGS cells, zinc oxide (ZnO) is used for the TCO. ZnO has a band gap of 3.3 eV.

To date, the industry standard in TCOs is ITO, or tin-doped indium-oxide. ITO has the drawback of being expensive. Indium, the film's primary metal, is rare (6000 metric tons worldwide in 2006), and its price fluctuates due to market demand (over $800 per kg in 2006). For this reason, doped binary compounds such as aluminum-doped zinc-oxide (AZO) and indium-doped cadmium-oxide have been proposed as alternative materials. AZO is composed of aluminum and zinc, two common and inexpensive materials, while indium-doped cadmium oxide only uses indium in low concentrations. In PV technology, except from ZnO many different TCOs have been used as transparent windows of the cell. These are the indium– tin oxide (ITO), the indium– gallium oxide (IGO) and SnO2.

### 3.4 BSF Layer

An effect is employed at the rear surface to minimize the impact of rear surface recombination velocity on voltage and current if the rear surface is closer than a diffusion length to the junction. A "back surface field" (BSF) consists of a higher doped region at the rear surface of the solar

cell. The interface between the high and low doped regions behaves like a p-n junction and an electric field forms at the interface which introduces a barrier to minority carrier flow to the rear surface. The minority carrier concentration is thus maintained at higher levels in the bulk of the device and the BSF has a net effect of passivating the rear surface. Now, taking the parameters of BSF layer from table 3.2 and changing the thickness of BSF layer from 100-500 nm the following outputs are found:

**Table-3.5**: BSF layer scaling comparison study of CdS CIGS solar cell for different doping concentration, where for all cases TCO layer = 50nm, front contact and back contact= 100nm, CdS=50nm, CIGS=300nm, TCO doping=$10^{20}$cm$^{-3}$.

| BSF layers (nm) | Concentration (cm$^{-3}$) | Voc (V) | Jsc (mA/cm$^2$) | Pmax (mW) | FF (%) | Efficiency (%) |
|---|---|---|---|---|---|---|
| 100 | CdS=1e17 CIGS=1e17 BSF=1e15 | 0.511 | 16.991 | 6.453 | 74.330 | 4.78 |
| | CdS=1e17 CIGS=1e17 BSF=1e16 | 0.524 | 17.665 | 7.000 | 75.631 | 5.294 |
| | CdS=1e17 CIGS=1e17 BSF=1e17 | 0.553 | 18.185 | 7.810 | 77.661 | 6.065 |
| 200 | CdS=1e17 CIGS=1e17 BSF=1e15 | 0.526 | 19.369 | 7.656 | 75 | 5.753 |
| | CdS=1e17 CIGS=1e17 BSF=1e16 | 0.540 | 19.941 | 8.282 | 76.909 | 6.370 |
| | CdS=1e17 CIGS=1e17 BSF=1e17 | 0.571 | 20.342 | 9.157 | 79 | 7.219 |
| 300 | CdS=1e17 CIGS=1e17 BSF=1e15 | 0.536 | 21.388 | 8.697 | 76 | 6.597 |
| | CdS=1e17 CIGS=1e17 BSF=1e16 | 0.552 | 21.902 | 9.369 | 77.49 | 7.261 |
| | CdS=1e17 CIGS=1e17 BSF=1e17 | 0.583 | 22.251 | 10.299 | 79 | 8.177 |

| | | | | | | |
|---|---|---|---|---|---|---|
| | CdS=1e17 CIGS=1e17 BSF=1e15 | 0.529 | 18.177 | 7.352 | 76 | 5.622 |
| 400 | CdS=1e17 CIGS=1e17 BSF=1e16 | 0.545 | 19.298 | 8.165 | 78 | 6.340 |
| | CdS=1e17 CIGS=1e17 BSF=1e17 | 0.584 | 20.799 | 9.692 | 80 | 7.733 |
| | CdS=1e17 CIGS=1e17 BSF=1e15 | 0.534 | 18.791 | 7.693 | 77 | 5.898 |
| 500 | CdS=1e17 CIGS=1e17 BSF=1e16 | 0.551 | 20.092 | 8.630 | 78 | 6.723 |
| | CdS=1e17 CIGS=1e17 BSF=1e17 | 0.591 | 21.833 | 10.325 | 80 | 8.261 |
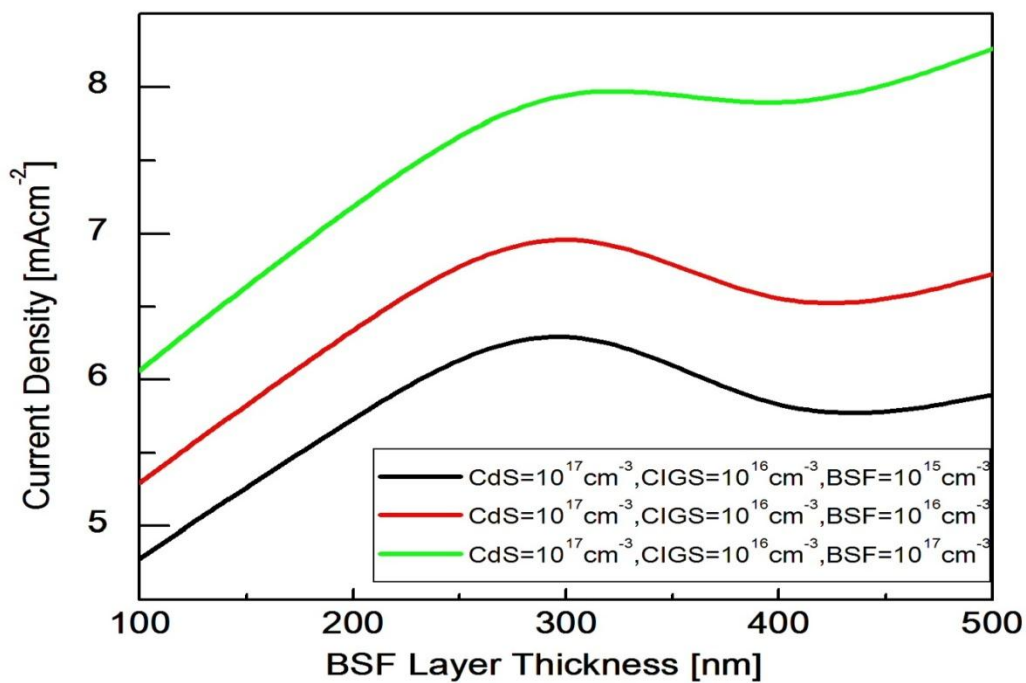


**Fig-3.2**: BSF layer Thickness vs Current density
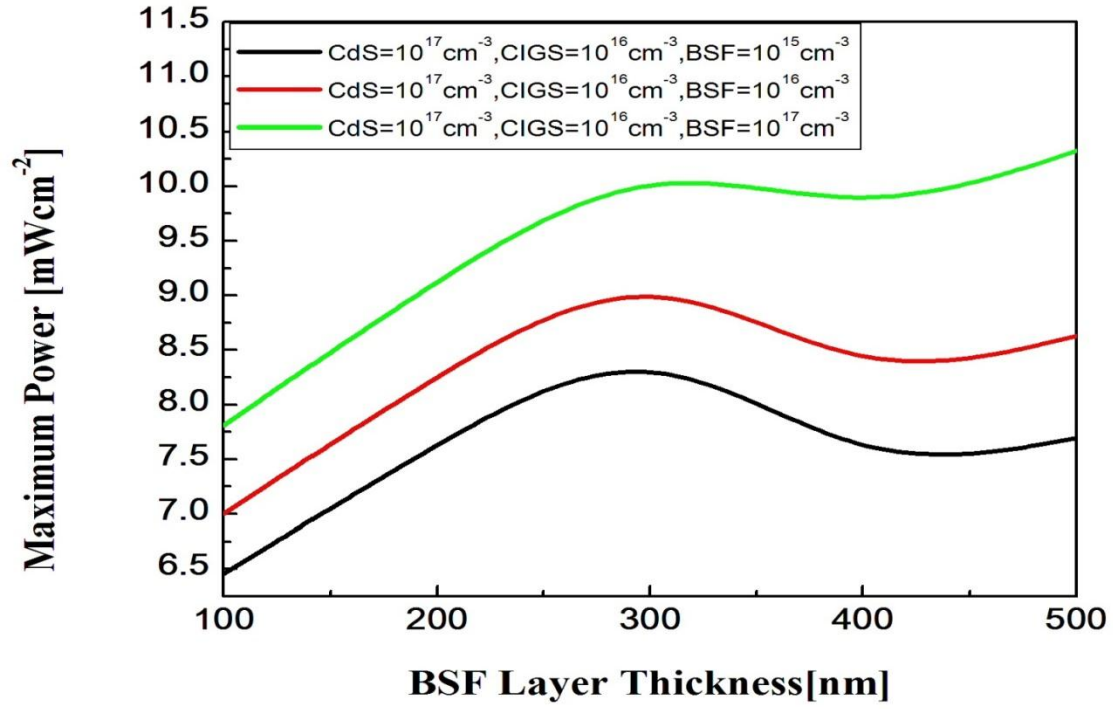
**Fig-3.3**: BSF layer Thickness vs Maximum Power
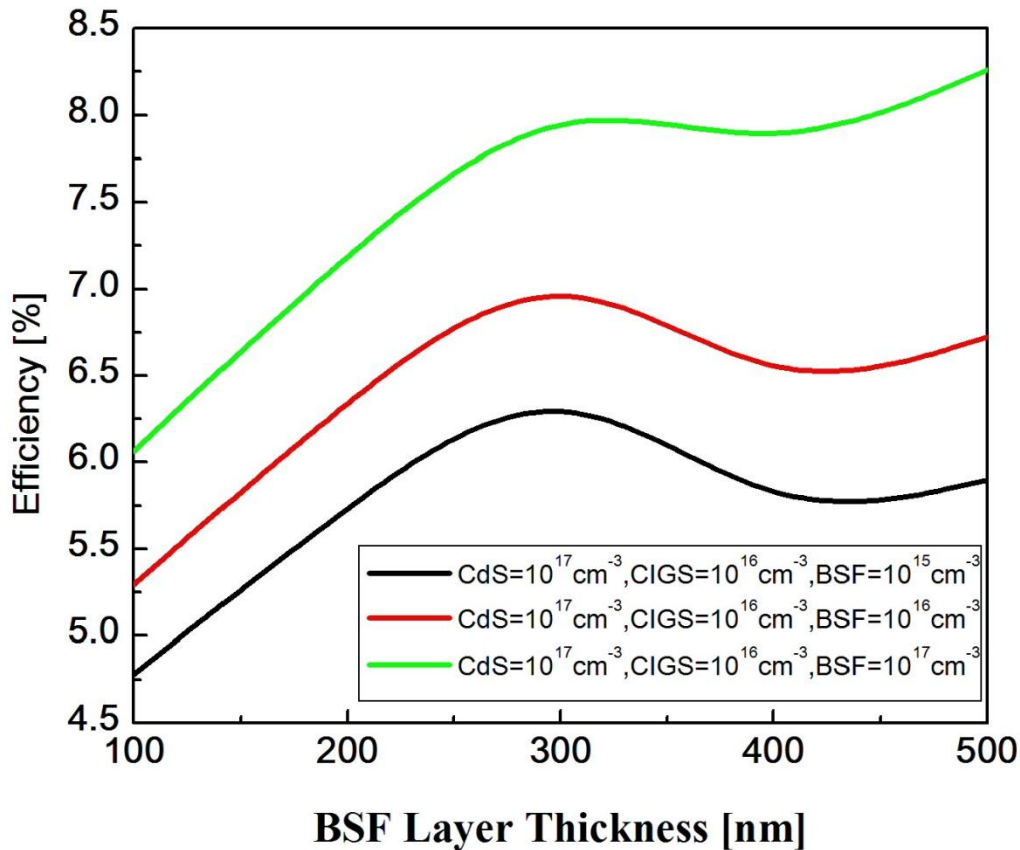
**Fig-3.4**: BSF layer Thickness vs Efficiency

The above figure shows the effect of BSF layer thickness on CdS-CIGS solar cell. The layer thickness is changed from 100 nm to 500nm.

## 3.5 Intrinsic Layer

PIN photodiodes are used in fiber optic network cards and switches. As a photo detector, the PIN diode is reverse biased. Under reverse bias, the diode ordinarily does not conduct (save a small dark current or leakage). When a photon of sufficient energy enters the depletion region of the diode, it creates an electron-hole pair. The reverse bias field sweeps the carriers out of the region creating a current. Some detectors can use avalanche multiplication. The same mechanism applies to the PIN structure, or p-i-n junction, of a solar cell. In this case, the advantage of usinga PIN structure over conventional semiconductor p–n junction is the better long wavelength

33

response of the former. In case of long wavelength irradiation, photons penetrate deep into the cell. But only those electron-hole pairs generated in and near the depletion region contribute to current generation. The depletion region of a PIN structure extends across the intrinsic region, deep into the device. This wider depletion width enables electron-hole pair generation deep within the device. This increases the quantum efficiency of the cell. The above three figures shows the efficiency, maximum power and current density versus I-layer thickness. We find that the efficiency, maximum power and current density are increases with increasing intrinsic layer thickness. Here we use variation in the thickness of I-layer and apply doping density $10^{17}$, $10^{17}$respectively at n-type, P-type and BSF layer doping densities are $10^{15}$ ,$10^{16}$, $10^{17}$.We get saturation at I layer thickness 1950nm. Finally we get the open circuit voltage 0.697 V, Fill factor 84 at 1950nm thickness of I-layer. At the back and font contact we use 100nm and for BSF 300nm.
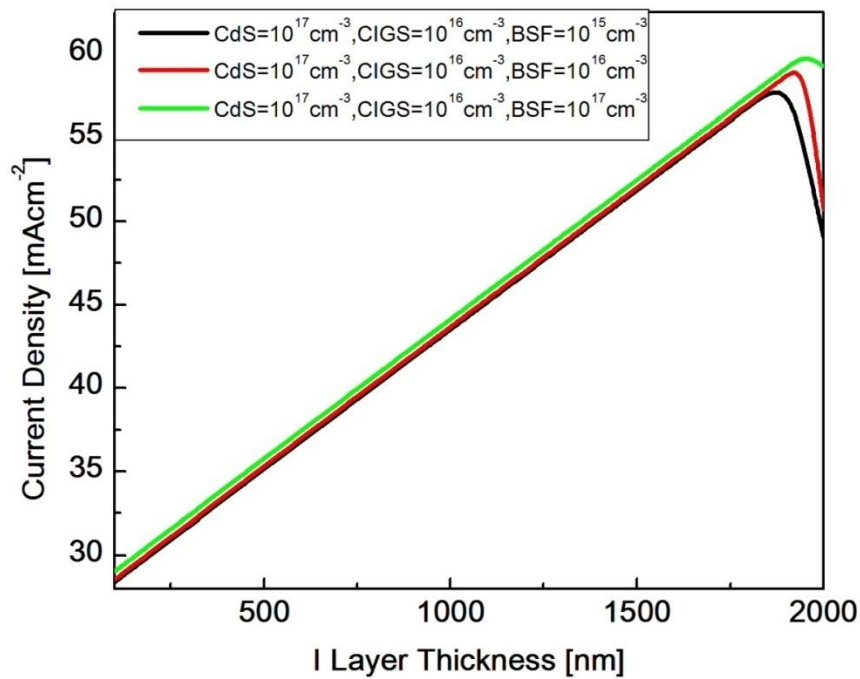


**Fig 3.5**: Current Density vs I Layer Thickness

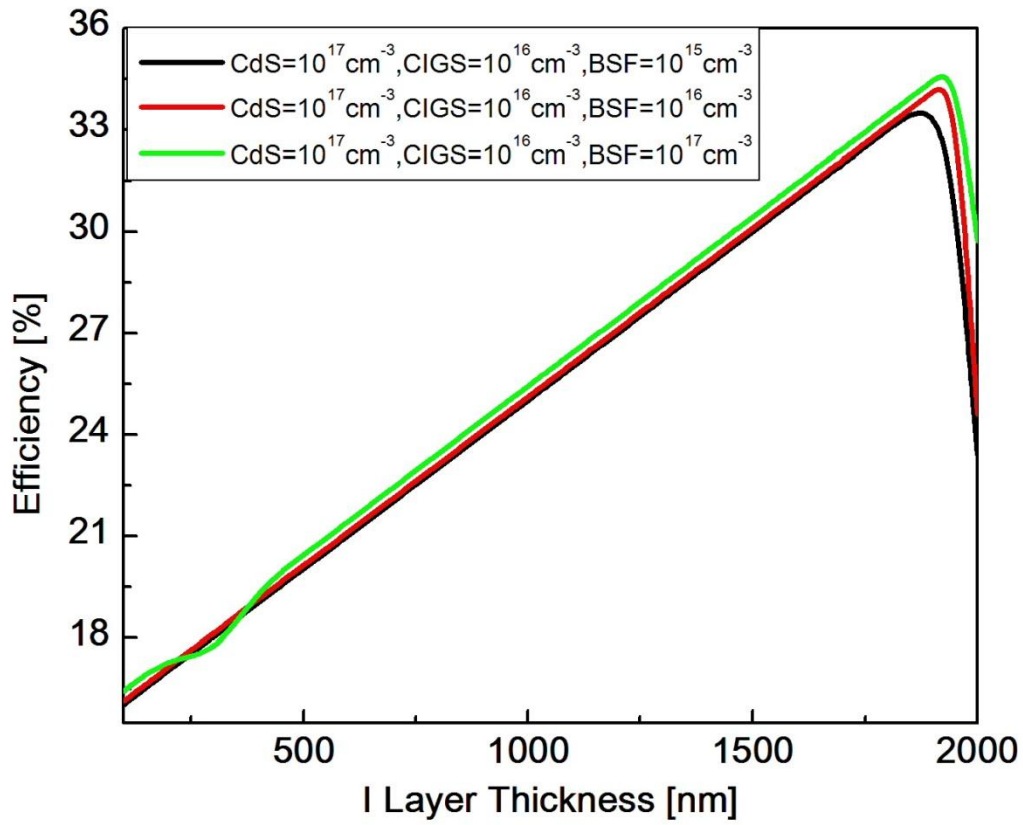Here, we get maximum current density 59.975 mA/cm$^2$ with the increase of I layer thickness.

**Fig 3.6**: Efficiency vs I Layer Thickness

Here, we get maximum efficiency 29.216% with the increase of I layer thickness.
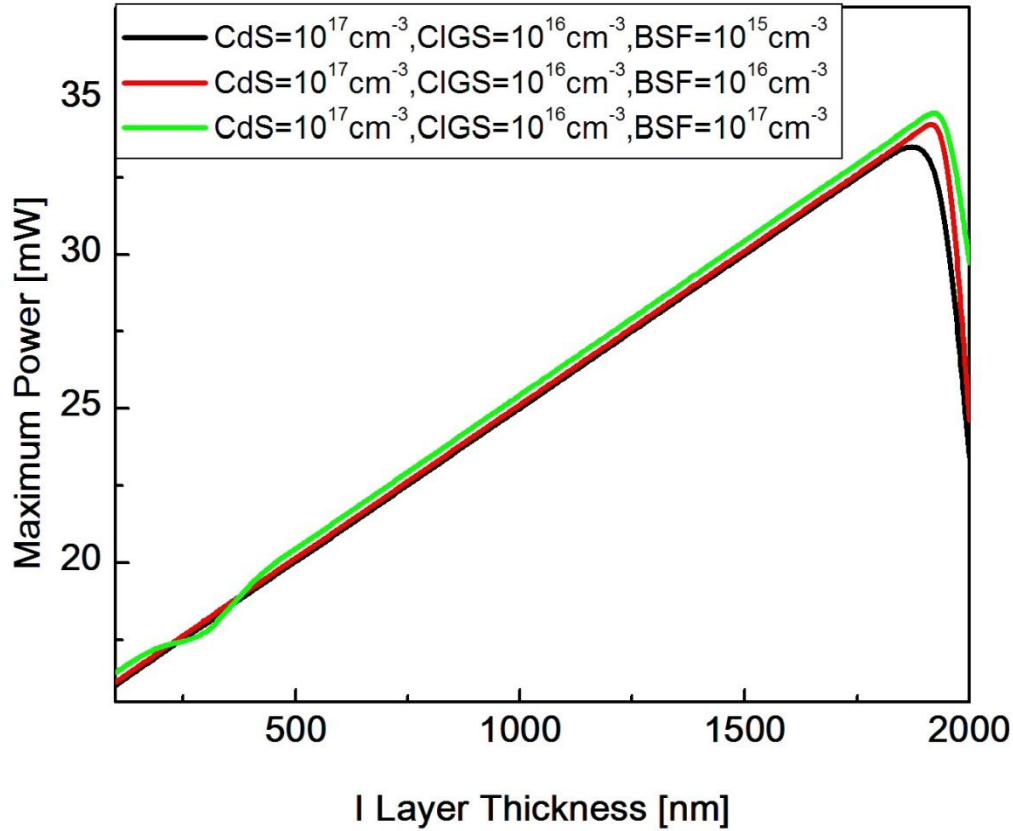
**Fig 3.7**: Maximum Power vs I Layer Thickness

Here, we get maximum power 34.945mW with the increase of I layer thickness.

## 3.6 P Layer

The above three figures shows the efficiency, maximum power and current density versus P-layer doping density. We find that the efficiency, maximum power and current density are decreases with increasing p layer doping density. Here we use variation in the doping density of P-layer and apply doping density $10^{17},10^{17}$ respectively at n-type, BSF. Finally we get the efficiency 29.500%, open circuit voltage 0.696 V, current density 60.790 mA/cm$^2$, fill factor 84, maximum power 35.329 mW at 1950nm thickness of I-layer, the back and font contact we use 100 nm and for BSF 300 nm.
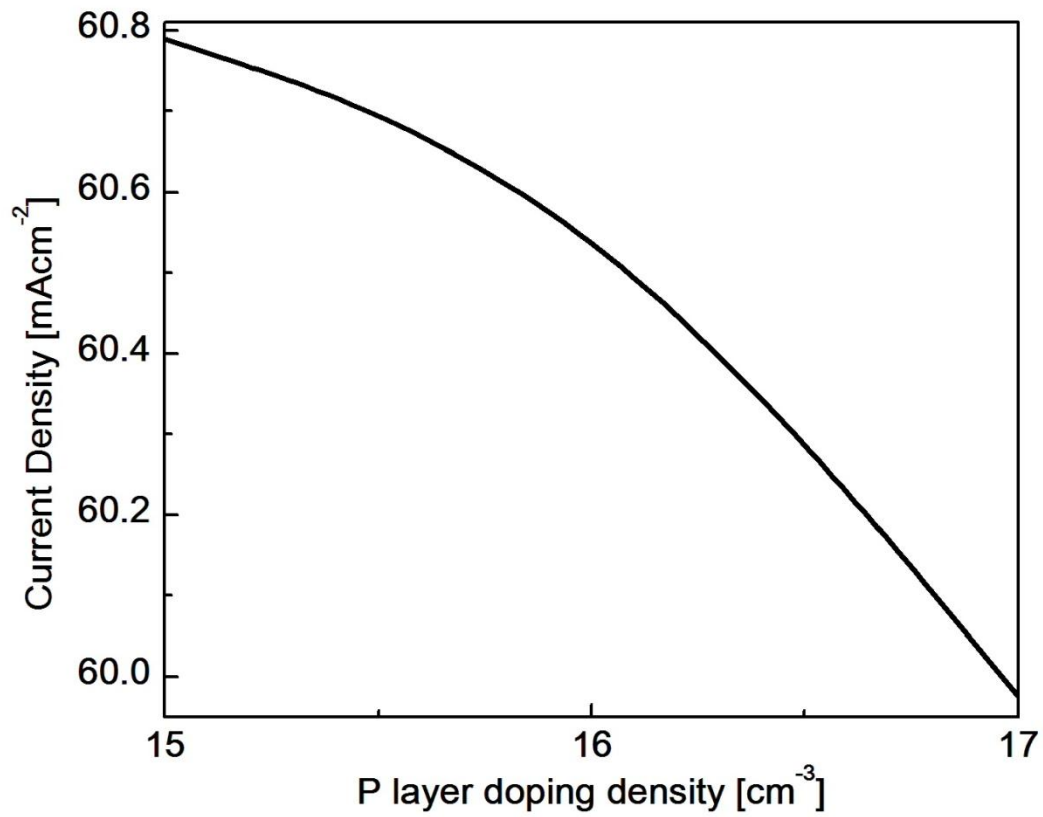
**Fig 3.8**: Current Density vs. P layer doping density

Here, we get maximum current density 60.790 mA/cm$^2$ with the decrease of doping density of Player.
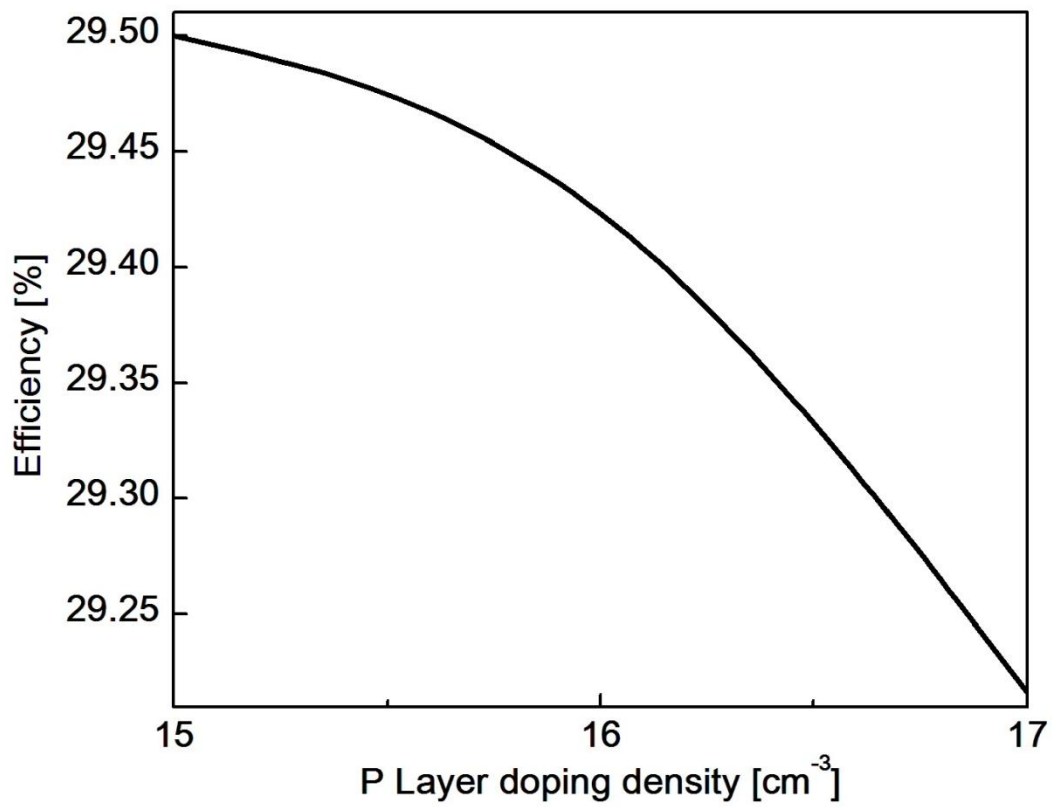
**Fig 3.9**: Efficiency vs. P layer doping density

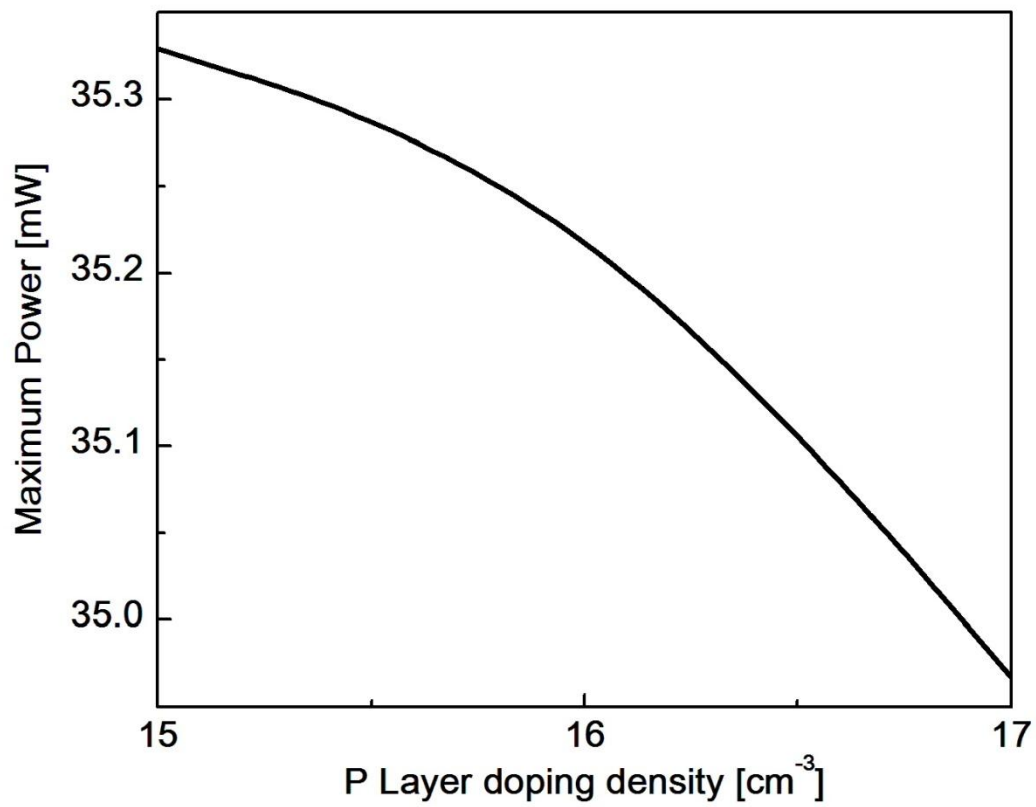Here, we get maximum efficiency 29.5%, with the decrease of doping density of P layer.

**Fig 3.10**: Maximum Power vs. P layer doping density

Here, we get maximum power 35.329 mWwith the decrease of doping density of P layer.

# Chapter 4

## Conclusions

In this project we designed and simulated a CdS/CIGS p-i-n high efficiency solar cell using SILVACO. We investigated the effects of i-layer thickness, BSF layer's thickness and doping density and p-layer's doping density on the cell performance. It is found that the efficiency of the solar is increased with the increase of thicknesses of intrinsic layer and BSF layer. The optimized thicknesses of TCO layer, n-layer, i-layer, p-layer and BSF layer are 50 nm, 200 nm, 1950 nm, 200 nm and 300 nm respectively. The cell efficiency, fill factor, maximum power, open circuit voltage and current density are found to be 29.5%, 84%, 35.329 mW, 0.696 Vand 60.79 mAcm$^{-2}$respectively.